

# Schwinger-Dyson equation in the complex plane

## – Two simple models –

Hidekazu TANAKA <sup>\*)</sup> and Shuji SASAGAWA  
Rikkyo University, Tokyo 171-8501, Japan

### ABSTRACT

Effective mass and energy are investigated using the Schwinger-Dyson equation (SDE) in the complex plane. As simple examples, we solve the SDE for the (1+1)-dimensional model and the strongly coupled quantum electrodynamics (QED). We also study some properties of the effective mass and energy in the complex plane.

---

<sup>\*)</sup> E-mail: tanakah@rikkyo.ac.jp

## §1. Introduction

The Schwinger-Dyson equation (SDE) [1,2] is one of the useful tools for evaluating non-perturbative phenomena. In many studies, the SDE is defined in Euclidean space. However, various extensions may be useful in computing the SDE, such as application to Minkowski space and extension to the complex momentum space.

One of the difficulties in calculation in Minkowski space is the presence of poles in the propagator. This requires knowledge of the precise pole positions of the propagator in the self-energy calculation. To avoid this, the Wick rotation from the real axis to the imaginary axis is often used in the momentum integration. However, the Wick rotation requires the location of the poles to be known in advance, but the value of an effective mass in non-perturbative region is non-trivial in calculation with the SDE. \*)

In order to study the properties of the propagators in non-perturbative region, the squared four-dimensional momentum has been extended to the complex value for the electron propagator in quantum electrodynamics (QED) [5,6] and the gluon propagator in QCD [7-9].

In this paper, we investigate a method, in which the mass and energy of the SDE are extended to the complex plane, and the propagator in the integrand of the self-energy is integrated with two different integral paths in the complex energy plane. Then we examine the properties of the solutions obtained by the SDE in the complex plane.

We explain our formulation and analysis method using two simple models. First, in order to illustrate our method, we examine a simple SDE for the effective mass which does not depend on the energy and momentum. This model in two-dimensions can be solved analytically and we compare these results with the numerically determined solutions obtained by the SDE. As a second model, we investigate the electron mass function in the strongly coupled QED with the instantaneous exchange approximation (IEA) [10,11], which is a slightly extended model of the first example.

Our paper is organized as follows: In Section 2, we formulate the SDE for the effective mass with a complex mass and energy for the first model. We discuss analytical solutions for the effective mass and energy in the complex plane with finite cutoff values of the momentum and we numerically calculate the effective mass and energy using the SDE. In Section 3, using the method presented in section 2, we investigate the SDE for the electron in the strongly coupled QED with the IEA. Section 4 is devoted to a summary and some comments. Explicit expressions of the complex mass and energy implemented in calculations are given in Appendix A. In Appendix B, we present a method to obtain the mass function in Minkowski space from the mass function obtained by the SDE in Euclidean space.

---

\*) A formal approach has been done in Refs.[3,4], in which the gluon propagator with complex singularities in Minkowski space is reconstructed starting from the Euclidean propagator by the analytic continuation.

## §2. The SDE for a simple model in the complex plane

In this section, we investigate a simple SDE for the effective mass  $M$  in order to illustrate our method. <sup>\*)</sup> The SDE for the effective mass is given as

$$M = i\lambda \int d^2Q \frac{M}{Q^2 - M^2 + i\varepsilon} = i\lambda \int dq_0 dq \frac{M}{q_0^2 - q^2 - M^2 + i\varepsilon} \quad (2.1)$$

with a momentum  $Q = (q_0, q)$ . Here,  $\lambda$  is a coupling constant.

The propagator in the integrand has poles, which satisfy  $Q^2 - M^2 + i\varepsilon = q_0^2 - q^2 - M^2 + i\varepsilon = 0$ .

In order to evaluate the effective mass in the complex plain, we extend  $q_0$  to a complex value  $z$  and the effective mass  $M$  is also extended to a complex value. Explicitly, they are written as  $z \equiv z_R + iz_I$  and  $M \equiv M_R + iM_I$ , respectively. Here, we write the denominator in the integrand as

$$z^2 - q^2 - M^2 + i\varepsilon \equiv z^2 - E^2(q) = (z - E(q))(z + E(q)), \quad (2.2)$$

where the complex energy  $E(q)$  is written as

$$E(q) \equiv E_R(q) + iE_I(q). \quad (2.3)$$

Therefore, the poles are located at  $z = \pm E(q)$  in the complex  $z$  plane. Here, we define  $E_R(q) > 0$ . Explicit relations among the complex values are given in Appendix A.

The SDE for the effective mass in terms of the complex values is written as

$$\begin{aligned} M &= i\lambda \int dq \oint_C dz \frac{M}{z^2 - q^2 - M^2(q) + i\varepsilon} \\ &= i\lambda \int dq \oint_C dz \frac{M}{(z - E(q))(z + E(q))}. \end{aligned} \quad (2.4)$$

Here, we write above equation as

$$M = \frac{1}{2}M^{(+)} + \frac{1}{2}M^{(-)}, \quad (2.5)$$

where

$$\begin{aligned} M^{(\pm)} &= i\lambda \int dq \oint_C dz \frac{1}{z - z_{\pm}} \left[ \frac{M}{z + z_{\pm}} \right] \\ &\equiv i\lambda \int dq \oint_C dz \frac{1}{z - z_{\pm}} f^{(\pm)}(z, q) \end{aligned} \quad (2.6)$$

with  $z_{\pm} = \pm E(q)$  and

$$f^{(\pm)}(z, q) = \frac{M}{z + z_{\pm}}. \quad (2.7)$$

---

<sup>\*)</sup> This example is a simplified model of the SDE for the effective mass of models with four-fermion interactions in (1+1)-dimensions, such as the Gross-Neveu model [12].

In our calculation, we integrate Eq.(2.6) around  $z = z_{\pm}$  with following two integral paths.

(1) Integral path including the imaginary axis

In this case, we separate the integral path around the poles  $z_{\pm} = \pm E(q)$  to  $C_1$  and  $C_2$  as follows:

For the integral path around  $z_+ = E(q)$ , we take  $-i\Lambda_0 \leq z \leq i\Lambda_0$  as the path  $C_1$ , and the path  $C_2$  is defined as clockwise rotation in right-half on the complex energy plane with  $z = \Lambda_0 e^{i\theta}$ , where we integrate the angle  $\theta$  from  $\theta = \pi/2$  to  $\theta = -\pi/2$ .

On the other hand, for the integral path around  $z_- = -E(q)$ , we take  $-i\Lambda_0 \leq z \leq i\Lambda_0$  as the path  $C_1$ , and the path  $C_2$  is defined as anticlockwise rotation in left-half on the complex energy plane with  $z = \Lambda_0 e^{i\theta}$ , where we integrate the angle  $\theta$  from  $\theta = \pi/2$  to  $\theta = 3\pi/2$ .

Integrating over the integral path  $C$  around the poles  $z_{\pm} = \pm E(q)$  in the right-hand side of Eq. (2.6), we have

$$M^{(\pm)} = i\lambda \int dq (\mp 2\pi i) f^{(\pm)}(z_{\pm}, q) = \pi\lambda \int dq \frac{M}{E(q)} \quad (2.8)$$

for  $\Lambda_0 \rightarrow \infty$ . Therefore, the SDE for the effective mass is given by

$$M = \frac{1}{2}M^{(+)} + \frac{1}{2}M^{(-)} = \pi\lambda \int dq \frac{M}{E(q)}. \quad (2.9)$$

This case corresponds to the SDE for the Euclidian momentum integration with the complex mass  $M$ , which is given as

$$M = \lambda \int dq \int_{-\infty}^{\infty} dq_4 \frac{M}{q_4^2 + q^2 + M^2 - i\varepsilon} \quad (2.10)$$

with  $z = iq_4$  in Eq. (2.4).\*)

(2) Integral path including the real axis

In this case, we separate the integral path around the poles  $z_{\pm} = \pm E(q)$  to  $C_1$  and  $C_2$  as follows:

For the integral path around  $z_+ = E(q)$ , we take  $-\Lambda_0 \leq z \leq \Lambda_0$  as the path  $C_1$ , and if  $E_1 > 0$ , the path  $C_2$  is defined as anticlockwise rotation in upper-half on the complex energy plane with  $z = \Lambda_0 e^{i\theta}$ , where we integrate the angle  $\theta$  from  $\theta = 0$  to  $\theta = \pi$ . If  $E_1 < 0$ , we take  $-\Lambda_0 \leq z \leq \Lambda_0$  as the path  $C_1$ , and the path  $C_2$  is defined as clockwise rotation in lower-half on the complex energy plane with  $z = \Lambda_0 e^{i\theta}$ , where we integrate the angle  $\theta$  from  $\theta = 0$  to  $\theta = -\pi$ .

For the integral path around  $z_- = -E(q)$ , we take  $-\Lambda_0 \leq z \leq \Lambda_0$  as the path  $C_1$ , and if  $E_1 < 0$ , the path  $C_2$  is defined as anticlockwise rotation in upper-half

---

\*) The contribution from the integral path  $C_2$  vanishes for  $\Lambda_0 \rightarrow \infty$ .

on the complex energy plane with  $z = \Lambda_0 e^{i\theta}$ , where we integrate the angle  $\theta$  from  $\theta = 0$  to  $\theta = \pi$ . If  $E_I > 0$ , we take  $-\Lambda_0 \leq z \leq \Lambda_0$  as the path  $C_1$ , and the path  $C_2$  is defined as clockwise rotation in lower-half on the complex energy plane with  $z = \Lambda_0 e^{i\theta}$ , where we integrate the angle  $\theta$  from  $\theta = 0$  to  $\theta = -\pi$ .

Integrating over the integral path  $C$  around the poles  $z_{\pm} = \pm E(q)$  in the right-hand side of Eq. (2.6), we have

$$\begin{aligned} M^{(\pm)} &= i\lambda \int dq (\pm 2\pi i) \left( \frac{E_I(q)}{|E_I(q)|} \right) f^{(\pm)}(z_{\pm}, q) \\ &= -\pi\lambda \int dq \left( \frac{E_I(q)}{|E_I(q)|} \right) \frac{M(q)}{E(q)} \end{aligned} \quad (2.11)$$

for  $\Lambda_0 \rightarrow \infty$ .

Therefore, the effective mass is given by

$$M = \frac{1}{2}M^{(+)} + \frac{1}{2}M^{(-)} = -\pi\lambda \int dq \left( \frac{E_I(q)}{|E_I(q)|} \right) \frac{M}{E(q)}. \quad (2.12)$$

This case corresponds to the SDE for the Minkowski momentum integration with the complex mass  $M$ , which is given as

$$M = i\lambda \int dq \int_{-\infty}^{\infty} dq_0 \frac{M}{q_0^2 - q^2 - M^2 + i\varepsilon} \quad (2.13)$$

with  $z = q_0$  in Eq. (2.4).

### 2.1. Analytical solutions

In this model, the effective mass does not depend on the momentum, and we can find analytical solutions for the SDE. Here, we write the SDE for the two integral paths (1) and (2) as

$$M = \pi s \lambda \int dq \frac{M}{E(q)} \quad (2.14)$$

with  $s = 1$  for the integral path (1) and  $s = -E_I(q)/|E_I(q)| = -[(M^2)_I - \varepsilon]/|(M^2)_I - \varepsilon|$  for the integral path (2), respectively.

From Eq.(2.14), the nontrivial solutions with  $M \neq 0$  are given by solving the equation

$$1 - \pi s \lambda \int dq \frac{1}{E(q)} = 0. \quad (2.15)$$

Thus, the real and imaginary parts of Eq.(2.15) satisfy

$$1 - \pi s \lambda \int dq \frac{E_R(q)}{|E(q)|^2} = 0 \quad (2.16)$$

and

$$\pi s \lambda \int dq \frac{E_I(q)}{|E(q)|^2} = 0, \quad (2.17)$$

respectively.

Here, Eq. (2.17) is written as

$$\pi s \lambda \int dq \frac{E_I(q)}{|E(q)|^2} = \pi s \lambda ((M^2)_I - \varepsilon) \int dq \frac{1}{2E_R(q)|E(q)|^2} = 0. \quad (2.18)$$

For  $E_R(q) > 0$ , we obtain  $(M^2)_I - \varepsilon = 0$  for  $s\lambda \neq 0$ , which gives  $E_I(q) = 0$ .\*)  
Moreover, from

$$(M^2)_I - \varepsilon = 2M_R M_I - \varepsilon = 0, \quad (2.19)$$

the imaginary part of the effective mass  $M_I$  is given by

$$M_I = \frac{\varepsilon}{2M_R}. \quad (2.20)$$

In the calculation below, we neglect the imaginary part of the effective mass for small  $\varepsilon$ . Thus, we approximate as  $(M^2)_R \simeq M_R^2$  for simplicity.

Using  $E_I(q) = 0$ , and introducing a ultraviolet cutoff  $\Lambda$  and an infrared cutoff  $\delta$  for the momentum  $q$ , we write Eq. (2.16) as

$$1 = \pi s \lambda \int_{-\Lambda}^{\Lambda} dq \frac{1}{E_R} \Theta(|q| - \delta) = 2\pi s \lambda \int_{\delta}^{\Lambda} dq \frac{1}{\sqrt{q^2 + M_R^2}}. \quad (2.21)$$

Here,  $\Theta(|q| - \delta)$  denotes the step function for restriction of the momentum  $q$ .

Eq. (2.21) gives

$$1 = 2\pi s \lambda \log \left| \frac{\Lambda + \sqrt{\Lambda^2 + M_R^2}}{\delta + \sqrt{\delta^2 + M_R^2}} \right|, \quad (2.22)$$

which is satisfied if  $s\lambda > 0$ . Therefore, for  $\lambda > 0$ ,  $s = -E_I(q)/|E_I(q)| = 1$  should be satisfied for the integral path (2).

Defining  $m_R = M_R/\Lambda$ ,  $\bar{\delta} = \delta/\Lambda$  and

$$\frac{1 + \sqrt{1 + m_R^2}}{\bar{\delta} + \sqrt{\bar{\delta}^2 + m_R^2}} = e^{1/(2\pi s \lambda)} \equiv \zeta \quad (2.23)$$

from Eq. (2.22), Eq. (2.23) is written as

$$m_R^2 (A m_R^2 - B) = 0 \quad (2.24)$$

with  $A = (1 - \zeta^2)^2$  and  $B = 4\zeta(1 - \bar{\delta}\zeta)(\zeta - \bar{\delta})$ .

The solution for  $m_R^2 \neq 0$  is given as

$$m_R^2 = \frac{B}{A} = \frac{4\zeta(1 - \bar{\delta}\zeta)(\zeta - \bar{\delta})}{(1 - \zeta^2)^2}. \quad (2.25)$$

---

\*) As shown in the next subsection,  $E_I(q)$  is determined by the asymptotic value, which is numerically calculated by the SDE with a given initial value of the mass  $M$ .

For  $s\lambda > 0$ ,  $\zeta - \bar{\delta} > 0$  is satisfied. Moreover,  $m_R^2 > 0$  demands  $1 - \bar{\delta}\zeta > 0$ , which gives

$$\zeta = e^{1/(2\pi s\lambda)} < \frac{1}{\bar{\delta}} = \frac{\Lambda}{\delta}. \quad (2.26)$$

Eq. (2.26) restricts the coupling constant  $\lambda$  as

$$\lambda > \frac{1}{2\pi \log \frac{\Lambda}{\delta}} \equiv \lambda_c \quad (2.27)$$

with  $s = 1$ .

For above restriction of  $\lambda$ , the real part of the effective mass is given as

$$m_R = \frac{M_R}{\Lambda} = \pm \sqrt{\frac{4\zeta(1 - \bar{\delta}\zeta)(\zeta - \bar{\delta})}{(1 - \zeta^2)^2}}. \quad (2.28)$$

## 2.2. Numerical solutions

In this subsection, we numerically calculate the effective mass and energy using the SDE for the two integral paths (1) and (2). The SDE is given in Eq. (2.14). In numerical calculation, we write the SDE for the real and imaginary parts of the effective mass as

$$M_R = 2\pi s\lambda \int_{\delta}^{\Lambda} dq \frac{[M(E(q))^*]_R}{|E(q)|^2} = 2\pi s\lambda \int_{\delta}^{\Lambda} dq \frac{M_R E_R(q) + M_I E_I(q)}{|E(q)|^2} \quad (2.29)$$

and

$$M_I = 2\pi s\lambda \int_{\delta}^{\Lambda} dq \frac{[M(E(q))^*]_I}{|E(q)|^2} = 2\pi s\lambda \int_{\delta}^{\Lambda} dq \frac{M_I E_R(q) - M_R E_I(q)}{|E(q)|^2}, \quad (2.30)$$

respectively with  $|E(q)|^2 = E_R^2(q) + E_I^2(q)$ . We solve the SDE by iteration method from some initial input values for the real and imaginary parts of the effective mass denoted by  $M_{R(0)}$  and  $M_{I(0)}$ .

For the integral path (1), we can start from any initial input values of the effective mass to solve the SDE, since  $s$  does not depend on the mass. However, for the integral path (2), the SDE has non-trivial solutions only for  $s = -E_I(q)/|E_I(q)| = -[(M^2)_I - \varepsilon]/[(M^2)_I - \varepsilon] = 1$ . Since  $(M^2)_I = 2M_R M_I$ , we set  $M_{R(0)}$  and  $M_{I(0)}$ , which satisfy  $(M^2)_{I(0)} = 2M_{R(0)} M_{I(0)} < 0$ .

In Fig.1, we present the convergence behaviors of  $|M|/\Lambda = \sqrt{M_R^2 + M_I^2}/\Lambda$  near the critical coupling constant  $\lambda_c$  denoted in Eq. (2.27) with  $\delta/\Lambda = 10^{-3}$ , which gives  $\lambda_c \simeq 0.023$ . Here, we set  $M_{R(0)} = -M_{I(0)} = 0.01\Lambda$ .\*)

From Fig.1, we can conclude that  $\lambda_c$  locates between  $\lambda = 0.020$  and  $\lambda = 0.025$ .

---

\*) We set  $\varepsilon = 10^{-5}\Lambda^2$ .

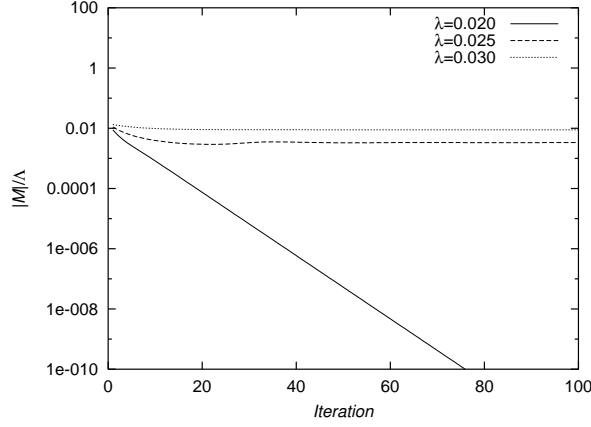


Fig. 1. The convergence behaviors of  $|M|/\Lambda$  for  $\lambda = 0.020, 0.025, 0.030$  with  $M_{R(0)} = -M_{I(0)} = 0.01\Lambda$ . The horizontal axis denotes the number of iterations.

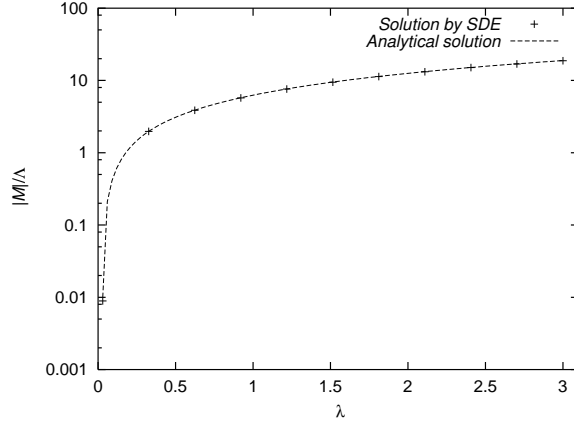


Fig. 2. The  $\lambda$  dependence of  $|M|/\Lambda$  for  $0.03 \leq \lambda \leq 3$  with  $M_{R(0)} = -M_{I(0)} = 0.01\Lambda$ . The dotted curve denotes the calculated result by the analytical solution divided by  $\Lambda$ .

In Fig.2, we present the  $\lambda$  dependence of the absolute value of the effective mass  $|M|/\Lambda$  for  $0.03 \leq \lambda \leq 3$  with  $M_{R(0)} = -M_{I(0)} = 0.01\Lambda$ . The dotted curve denotes the calculated result using Eqs. (2.20) and (2.28).

In the following calculations, we set four initial input values for the effective mass as  $M_{R(0)} = \pm 0.01\Lambda$  and  $M_{I(0)} = \pm 0.01\Lambda$ , respectively, for  $\lambda = 0.3$ .

In Figs.3 and 4, we show the convergence behaviors of the real and imaginary parts of the energy with the momentum  $q = 0$ , respectively. The straight lines denote the energy calculated using the analytical solutions of the effective mass given in Eqs.(2.20) and (2.28).(See Appendix A.)

Since the real part of the energy is defined to be positive, the numerical results do not depend on the signs of initial input values of the effective mass. The imaginary part of the energy converges as  $E_I \rightarrow 0$ , in which the convergence behavior depends on the respective signs of  $(M^2)_{I(0)}$ . The calculated results shown in Figs. 1-4 are



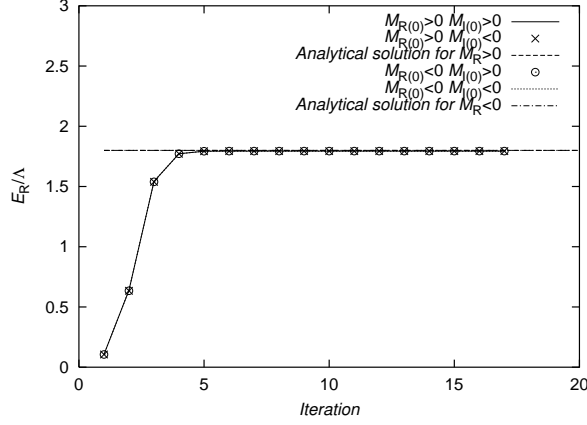


Fig. 3. The convergence behaviors of  $E_R(q)/\Lambda$  with  $q = 0$ . The straight lines denote the energy divided by  $\Lambda$  calculated using the analytical solutions of the effective mass. The horizontal axis denotes the number of iterations.

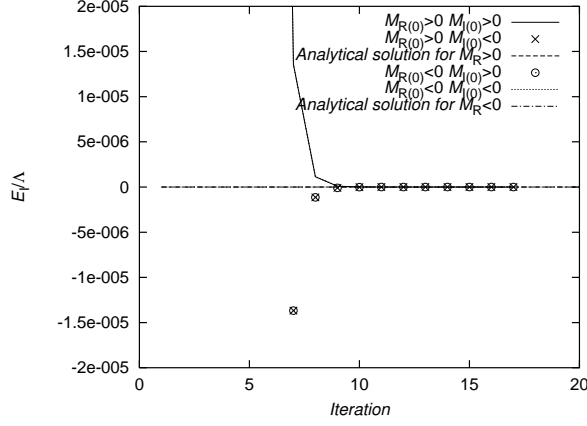


Fig. 4. The convergence behaviors of  $E_I(q)/\Lambda$  with  $q = 0$ . The straight lines denote the analytical solutions of the energy, which is  $E_I(q)/\Lambda = 0$ . The horizontal axis denotes the number of iterations.

common for the two integral paths (1) and (2).

On the other hand, the convergence behaviors of the effective mass are different for the two integral paths.

For the integral path (1), the real and imaginary parts of the effective mass calculated by the SDE are shown in Figs.5 and 6, respectively. As shown in Fig. 5, the convergent solutions split into two values depending on the respective signs of  $M_{R(0)}/\Lambda$ . As shown in Fig.6, the imaginary part of the effective mass is small and it depends on  $\varepsilon$ . Moreover,  $M_I/\Lambda$  initially behaves according to the sign of each  $M_{I(0)}/\Lambda$ , but the convergent solutions depend on the respective signs of  $M_{R(0)}/\Lambda$ .

For the integral path (2), the convergence behaviors of the effective mass calculated by the SDE are shown in Figs.7 and 8, respectively. As shown in Figs. 7 and

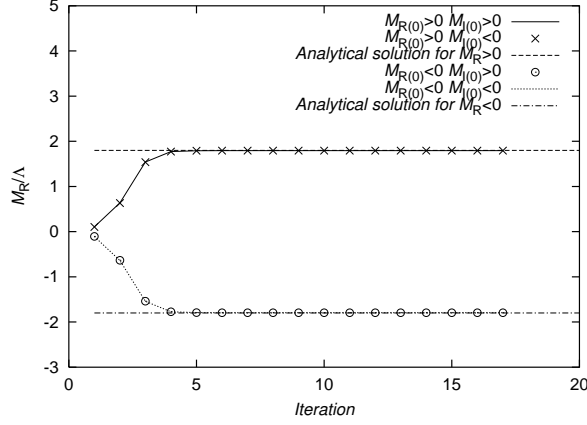


Fig. 5. The convergence behaviors of  $M_R/\Lambda$  for the integral path (1). The straight lines denote the analytical solutions of the real part of the effective mass divided by  $\Lambda$ . The horizontal axis denotes the number of iterations.

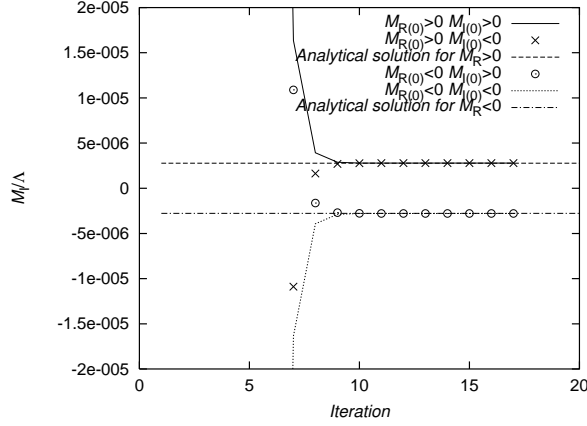


Fig. 6. The convergence behaviors of  $M_I/\Lambda$  for the integral path (1). The straight lines denote the analytical solutions of the imaginary part of the effective mass divided by  $\Lambda$ . The horizontal axis denotes the number of iterations.

8, the convergent solutions split into two values depending on the respective signs of  $M_{R(0)}/\Lambda$  for  $(M^2)_{I(0)} < 0$ . However, for  $(M^2)_{I(0)} > 0$ , the iterated values are oscillated.

### §3. The strong coupling QED with the IE approximation

#### 3.1. The SDE for the electron mass function

In this section, we consider a slightly more non-trivial example, the strongly coupled QED.

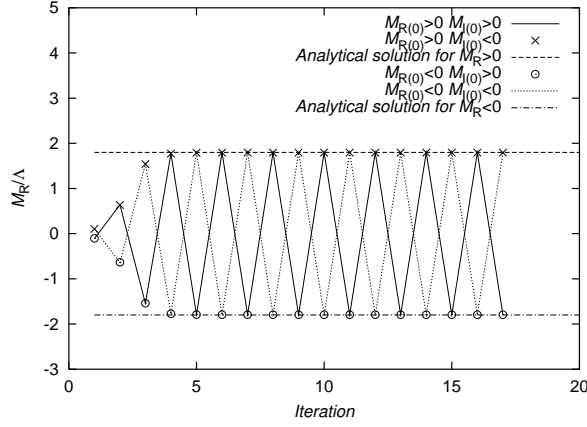


Fig. 7. The convergence behaviors of  $M_R/\Lambda$  for the integral path (2). The straight lines denote the analytical solutions of the real part of the effective mass divided by  $\Lambda$ . The horizontal axis denotes the number of iterations.

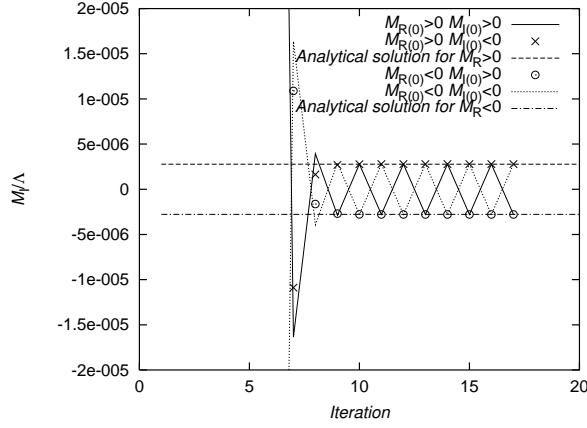


Fig. 8. The convergence behaviors of  $M_I/\Lambda$  for the integral path (2). The straight lines denote the analytical solutions of the imaginary part of the effective mass divided by  $\Lambda$ . The horizontal axis denotes the number of iterations.

We write the self-energy of the electron as

$$\Sigma(P) = a(P)\not{P} + b(P) \quad (3.1)$$

with a four-dimensional momentum  $P = (p_0, \mathbf{p})$ , which is given by

$$-i\Sigma(P) = (-ie)^2 \int \frac{d^4Q}{(2\pi)^4} \gamma^\mu iS(Q) \Gamma^\nu iD_{\mu\nu}(K), \quad (3.2)$$

in one-loop approximation. Here,  $S(Q)$  and  $D_{\mu\nu}(K)$  are propagators of a electron with  $Q = (q_0, \mathbf{q})$  and that of a photon with  $K = (k_0, \mathbf{k}) = P - Q = (p_0 - q_0, \mathbf{p} - \mathbf{q})$ , respectively

The effective propagator of the electron is given by

$$iS(Q) = \frac{i}{Q - \Sigma(Q) + i\varepsilon} = \frac{i}{(1 - a(Q))Q - b(Q) + i\varepsilon} \quad (3.3)$$

with a massless electron. For simplicity, we take  $\Sigma(P) = b(P) \equiv M(P)$  with  $a(P) = 0$  and the electron-photon vertex with  $\Gamma_\mu = \gamma_\mu$  in the Landau gauge. Here, the photon propagator in the Landau gauge with quenched approximation is given as

$$iD_{\mu\nu}(K) = \left( -g_{\mu\nu} + \frac{K_\mu K_\nu}{K^2} \right) \frac{i}{K^2 + i\varepsilon}. \quad (3.4)$$

Using the approximation described above, the mass function is given by

$$M(P) = \frac{1}{4} \text{Tr}[\Sigma(P)] = ie^2 \int \frac{d^4 Q}{(2\pi)^4} \frac{-3M(Q)}{Q^2 - M^2(Q) + i\varepsilon} \frac{1}{K^2 + i\varepsilon}. \quad (3.5)$$

In the following calculations, we use the instantaneous exchange approximation (IEA) as  $k_0 = 0$ , in which the mass function does not depend on  $p_0$  and  $q_0$ .

Integrating over the angle of the momentum  $\mathbf{q}$ , we obtain the SDE with the IEA as

$$M(p) = i \frac{3\alpha}{4\pi^2} \int_\delta^A dq \frac{q}{p} \int dq_0 \frac{M(q)}{q_0^2 - q^2 - M^2(q) + i\varepsilon} \int_{\eta_-^2}^{\eta_+^2} \frac{dk^2}{k^2 - i\varepsilon} \quad (3.6)$$

with  $p = |\mathbf{p}|$ ,  $q = |\mathbf{q}|$ ,  $k = |\mathbf{k}|$ ,  $\alpha = e^2/(4\pi)$  and  $\eta_\pm^2 = (p \pm q)^2$ , respectively. Using

$$I(q) \equiv i \int dq_0 \frac{1}{q_0^2 - q^2 - M^2(q) + i\varepsilon} = i \int dq_0 \frac{1}{(q_0 - E(q))(q_0 + E(q))}, \quad (3.7)$$

we can write the SDE as

$$M(p) = \frac{3\alpha}{4\pi^2} \int_\delta^A dq \frac{q}{p} M(q) I(q) \int_{\eta_-^2}^{\eta_+^2} \frac{dk^2}{k^2 - i\varepsilon}. \quad (3.8)$$

Extending the  $M(p)$ ,  $M(q)$  and  $q_0$  to the complex values, we can evaluate  $I(q)$  by the method in the previous section, which is given as

$$I(q) = s(q) \pi \frac{1}{E(q)} \quad (3.9)$$

with  $s(q) = 1$  for the integral path (1) and  $s(q) = -E_I(q)/|E_I(q)|$  for the integral path (2), respectively. Therefore, the SDE for the mass function is given by

$$M(p) = \frac{3\alpha}{4\pi} \int_\delta^A dq \frac{q}{p} s(q) M(q) \frac{1}{E(q)} \int_{\eta_-^2}^{\eta_+^2} \frac{dk^2}{k^2 - i\varepsilon}. \quad (3.10)$$

Integrating over  $k^2$  in Eq.(3.10), we have

$$J(p, q) \equiv \int_{\eta_-^2}^{\eta_+^2} \frac{dk^2}{k^2 - i\varepsilon} \equiv J_R(p, q) + iJ_I(p, q) \quad (3.11)$$

with

$$J_R(p, q) = \frac{1}{2} \log \frac{\eta_+^4 + \varepsilon^2}{\eta_-^4 + \varepsilon^2} \quad (3.12)$$

and

$$J_I(p, q) = \arctan \frac{\eta_+^2}{\varepsilon} - \arctan \frac{\eta_-^2}{\varepsilon}, \quad (3.13)$$

respectively.

Therefore, the SDE for the mass function is given by

$$M(p) = \frac{3\alpha}{4\pi} \int_{\delta}^{\Lambda} dq \frac{q}{p} s(q) \frac{M(q)E^*(q)}{|E(q)|^2} J(p, q). \quad (3.14)$$

From the above formula, the real and imaginary parts of  $M(p)$  are given by

$$\begin{aligned} M_R(p) &= \frac{3\alpha}{4\pi} \int_{\delta}^{\Lambda} dq \frac{q}{p} s(q) \frac{[M(q)E^*(q)J(p, q)]_R}{|E(q)|^2} \\ &= \frac{3\alpha}{4\pi} \int_{\delta}^{\Lambda} dq \frac{q}{p} s(q) \frac{[M(q)E^*(q)]_R J_R(p, q) - [M(q)E^*(q)]_I J_I(p, q)}{|E(q)|^2} \end{aligned} \quad (3.15)$$

and

$$\begin{aligned} M_I(p) &= \frac{3\alpha}{4\pi} \int_{\delta}^{\Lambda} dq \frac{q}{p} s(q) \frac{[M(q)E^*(q)J(p, q)]_I}{|E(q)|^2} \\ &= \frac{3\alpha}{4\pi} \int_{\delta}^{\Lambda} dq \frac{q}{p} s(q) \frac{[M(q)E^*(q)]_R J_I(p, q) + [M(q)E^*(q)]_I J_R(p, q)}{|E(q)|^2} \end{aligned} \quad (3.16)$$

with

$$[M(q)E^*(q)]_R = M_R(q)E_R(q) + M_I(q)E_I(q) \quad (3.17)$$

and

$$[M(q)E^*(q)]_I = M_I(q)E_R(q) - M_R(q)E_I(q), \quad (3.18)$$

respectively.

### 3.2. Numerical results

As can be seen in the previous example, it is possible to use the SDE for the integral path (1) to find the poles of the effective propagator. Therefore, we present the results only for the integral path (1). Here, we show the convergence behaviors of the real and imaginary parts of the energy described by  $E_R(p)$  and  $E_I(p)$  with the momentum  $p = \delta$ ,  $\alpha = 1$ ,  $\delta/\Lambda = 10^{-3}$  and  $\varepsilon/\Lambda^2 = 10^{-4}$ .\*)

---

\*)  $E_R(p)$  and  $E_I(p)$  are calculated using  $M_R(p)$  and  $M_I(p)$  obtained by the SDE.

In the following calculations, we set four initial input values for the mass functions as  $M_{R(0)} = \pm 0.01\Lambda$  and  $M_{I(0)} = \pm 0.01\Lambda$ , respectively.

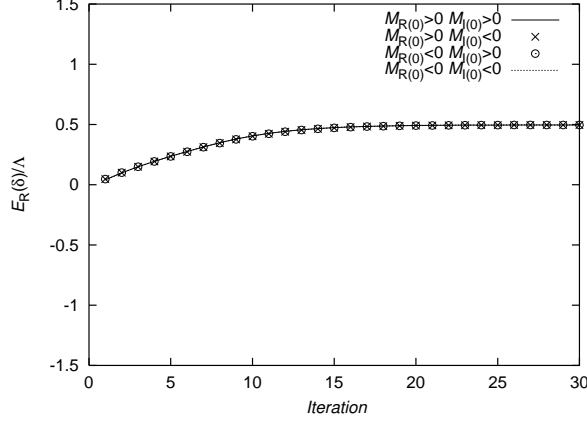


Fig. 9. The convergence behaviors of  $E_R(p)/\Lambda$  with  $p = \delta$ . The horizontal axis denotes the number of iterations.

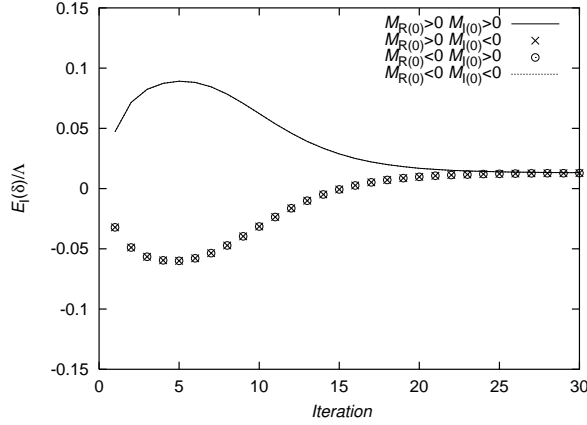


Fig. 10. The convergence behaviors of  $E_I(p)/\Lambda$  with  $p = \delta$ . The horizontal axis denotes the number of iterations.

In Fig.9, since the real part of the energy is defined to be positive, the numerical results do not depend on the signs of initial input values of the mass function. In Fig.10, the imaginary part of the energy converges to  $E_I(\delta) > 0$ , in which the convergence behaviors depend on the respective signs of  $(M^2)_{I(0)}$ .<sup>\*)</sup>

The real and imaginary parts of the mass function calculated by the SDE with  $p = \delta$  are shown in Figs.11 and 12, respectively. As shown in Fig. 11, the convergent solutions split into two values depending on the respective signs of  $M_{R(0)}/\Lambda$ .

---

<sup>\*)</sup> In the numerical calculations, we rejected the integral point  $p = q$ , which corresponds to the infrared singular point for the photon propagator.

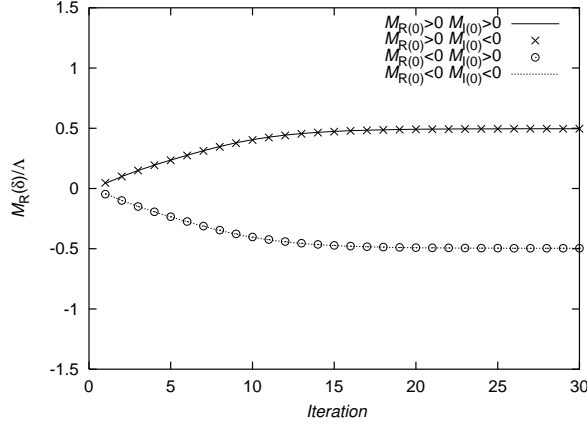


Fig. 11. The convergence behaviors of  $M_R(p)/\Lambda$  with  $p = \delta$ . The horizontal axis denotes the number of iterations.

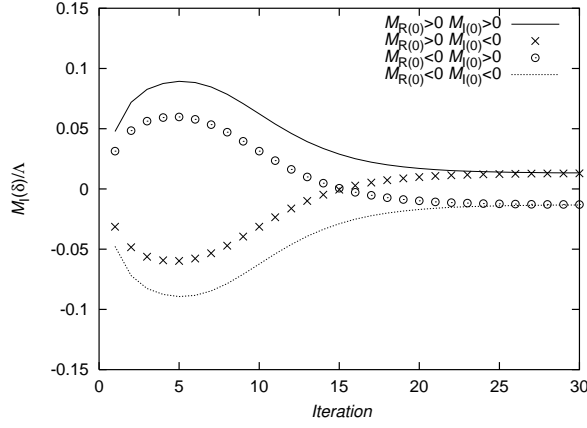


Fig. 12. The convergence behaviors of  $M_I(p)/\Lambda$  with  $p = \delta$ . The horizontal axis denotes the number of iterations.

As shown in Fig.12,  $M_I(\delta)/\Lambda$  initially behaves according to the sign of each  $M_{I(0)}/\Lambda$ , but the convergent solution depends on the respective signs of  $M_{R(0)}/\Lambda$ . The behaviors shown above are similar to those for the first model in the previous section.

In Fig.13, we present the location of the poles of the effective propagator with  $\alpha = 1$ ,  $\delta/\Lambda = 10^{-3}$  and  $\varepsilon/\Lambda^2 = 10^{-4}$  from  $p = \delta$  to  $p = \Lambda$ , in which the denominator of the effective propagator is defined as

$$D(y, p) = y^2 - p^2 - M^2(p) + i\varepsilon = (y - E(p))(y + E(p)) \quad (3.19)$$

with  $y = y_R + iy_I$ . The arrows denote the momentum dependence of the poles of the effective propagator.

As shown in Fig.13, since  $E_I(p) > 0$  for  $\delta \leq p \leq \Lambda$ , the solution obtained by the SDE in Eq.(3.14) with  $s(q) = -E_I(q)/|E_I(q)|$  for the integral path (2) may oscillate. In Appendix B, we present an alternative method to obtain the mass function in

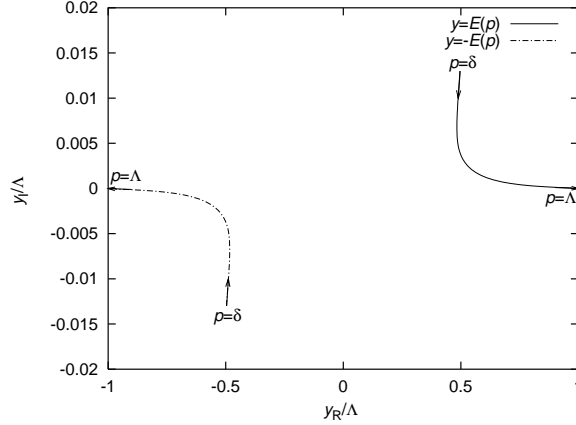


Fig. 13. The location of the poles of the effective propagator with  $\alpha = 1$  and  $\varepsilon/\Lambda^2 = 10^{-4}$  from  $p = \delta$  to  $p = \Lambda$ .

Minkowski space, in which we use Eq.(3.14) with  $s(q) = -E_I(q)/|E_I(q)|$ . However, in order to evaluate the right-hand side of Eq.(3.14), we use the solution of the mass function  $M_{(E)}(p)$  obtained by the SDE for the integral path (1). In our present case, the mass function  $M_{(M)}(p)$  in Minkowski space is given as  $M_{(M)}(p) = -M_{(E)}(p)$ . Therefore, the relation between the energy  $E_{(M)}(p)$  in Minkowski space and the energy  $E_{(E)}(p)$  in Euclid space is given as  $E_{(M)}(p) = E_{(E)}(p)$ .

#### §4. Summary and Comments

In this paper, we investigated a method, in which the mass and energy of the Schwinger-Dyson equation (SDE) are extended to the complex plane, and the propagator in the integrand of the self-energy is integrated with two different integral paths in the complex energy plane. Then we examined the properties of the solutions obtained by the SDE in the complex plane.

We explained our formulation and analysis method using two simple examples. First, in order to illustrate our method, we examined a simple SDE for the effective mass which does not depend on the energy and momentum. We solved this model analytically and compared with the numerically determined solutions obtained by the SDE. Then we compared the effective mass and energy calculated in two different integral paths in the complex energy plane. First, we investigated the effect of the momentum cutoff for the effective mass. Though the infrared cutoff  $\delta$  on the momentum is an artificial parameter for numerical calculations, this example suggests a possibility of changing the critical point in physical systems with restricted low-momentum region. In this model, the imaginary part of the energy is zero and the poles of the effective propagator are on the real axis, which is different situation in the strongly coupled quantum electrodynamics (QED) and the quantum chromodynamics (QCD) pointed out in Ref.[5-9], in which the poles are not on the real axis.

We also investigated the dependence of the solutions obtained by the SDE on



the initial input values. The effective mass obtained by the SDE depends on the respective signs of the initial input values. From our calculations, the SDE may lead to multiple solutions depending on the initial input values. Moreover, for the integral path including the real axis, the sign of effective mass is not determined for some initial input values. These results suggest that the calculation of the SDE requires careful choice of the initial input values.

As a second example, we investigated the strongly coupled QED with the instantaneous exchange approximation (IEA). In this model, the mass function depends on the momentum.

We found that the imaginary part of the energy  $E_I$  is positive value over the defined momentum range. Although  $E_I$  decreases as  $E_I \rightarrow +0$  for  $E_R > 0$  with  $\varepsilon \rightarrow +0$ , the effective propagator has poles which are different from the pole locations in the usual Feynman propagator, where  $E_I = -\varepsilon \rightarrow -0$  for  $E_R > 0$  with  $\varepsilon \rightarrow +0$ . The pole location of the Feynman propagator relates to the time-evolution of particle propagation. For example, a positive energy solution of particle propagates forward in time. In our case, the relation with the time-ordered product of the wave-function in the definition of the two-point Green's function of the Feynman propagator appears to be broken. If we take the Fourier transform of our modified propagator from momentum space to space-time, for the positive (negative) energy solution, we integrate over the upper (lower) half of the complex energy plane converging for time  $t < 0$  ( $t > 0$ ). Therefore, we have a propagator for positive (negative) energy solution which is defined in  $t < 0$  ( $t > 0$ ). From our example, it may be expected that the effective propagator behaves anomalously in non-perturbative region.

In order to get more practical results, we need to investigate the mass function, which depends on the energy component of the four-dimensional momentum. The way to do this is to calculate the self-energy without the IEA.

Although our models studied in this paper may be a little too simple for real physical situations, we expect that our method and analyses will give some hints when applying the SDE to other models such as QCD in non-perturbative region.

## Appendix A. Complex mass and energy

In order to solve the SDE in complex energy plane, we need the explicit forms of the complex mass and energy.

We define the complex mass as  $M = M_R + iM_I$  and the squared of the mass as  $M^2 = (M^2)_R + i(M^2)_I$ . Here,  $(M^2)_R$  and  $(M^2)_I$  are given by

$$(M^2)_R = M_R^2 - M_I^2, \quad (M^2)_I = 2M_R M_I.$$

The squared energy  $E^2$  is defined by

$$E^2 = q^2 + M^2 - i\varepsilon \equiv (E^2)_R + i(E^2)_I.$$

with

$$(E^2)_R = q^2 + (M^2)_R, \quad (E^2)_I = (M^2)_I - \varepsilon.$$

On the other hand, using the complex energy  $E = E_R + iE_I$ ,  $(E^2)_R$  and  $(E^2)_I$  are written as

$$(E^2)_R = E_R^2 - E_I^2, \quad (E^2)_I = 2E_R E_I.$$

Therefore the imaginary part of the energy is given by

$$E_I = \frac{(E^2)_I}{2E_R}.$$

Substituting above equation to  $(E^2)_R = E_R^2 - E_I^2$ , we have a quadratic equation for  $E_R^2$  as

$$(E_R^2)^2 - E_R^2(E^2)_R - (E^2)_I^2/4 = 0.$$

The solution of the equation for  $E_R^2 > 0$  is given by

$$E_R^2 = \frac{(E^2)_R + |E^2|}{2}$$

with  $|E^2| = \sqrt{[(E^2)_R]^2 + [(E^2)_I]^2}$ .

Therefore, we get  $E_R$  and  $E_I$  as

$$E_R = \sqrt{\frac{(E^2)_R + |E^2|}{2}}, \quad E_I = \frac{(E^2)_I}{2E_R}$$

for  $E_R > 0$ .

## Appendix B. Alternative method to evaluation the mass function in Minkowski space

Here, the SDE with IEA in the complex plane is given as

$$\begin{aligned} M(p) &= i \frac{3\alpha}{4\pi^2} \int dq \frac{q}{p} \oint dz \frac{M(q)}{z^2 - q^2 - M^2(q) + i\varepsilon} \int_{\eta_-^2}^{\eta_+^2} \frac{dk^2}{k^2 - i\varepsilon} \\ &\equiv \frac{3\alpha}{4\pi^2} \int dq \frac{q}{p} M(q) I(q) \int_{\eta_-^2}^{\eta_+^2} \frac{dk^2}{k^2 - i\varepsilon} \end{aligned}$$

with

$$I(q) = i \oint dz \frac{1}{z^2 - q^2 - M^2(q) + i\varepsilon} = i \oint dz \frac{1}{(z - E(q))(z + E(q))},$$

where  $M(p)$ ,  $M(q)$ ,  $E(q)$  and  $z$  are the complex values. Defining

$$\begin{aligned} I_{(M)}(q) &\equiv i \int_{-\infty}^{\infty} dq_0 \frac{1}{q_0^2 - q^2 - M^2(q) + i\varepsilon}, \\ I_{(E)}(q) &\equiv i \int_{-\infty}^{\infty} idq_4 \frac{1}{-q_4^2 - q^2 - M^2(q) + i\varepsilon} = \int_{\infty}^{-\infty} dq_4 \frac{1}{q_4^2 + q^2 + M^2(q) - i\varepsilon}, \end{aligned}$$

$$I_{(C_+)}(q) \equiv \lim_{\Lambda_0 \rightarrow \infty} i \int_0^{\pi/2} id\theta \frac{\Lambda_0 e^{i\theta}}{(\Lambda_0 e^{i\theta})^2 - q^2 - M^2(q) + i\varepsilon}$$

and

$$I_{(C_-)}(q) \equiv \lim_{\Lambda_0 \rightarrow \infty} i \int_{3\pi/2}^{\pi} id\theta \frac{\Lambda_0 e^{i\theta}}{(\Lambda_0 e^{i\theta})^2 - q^2 - M^2(q) + i\varepsilon},$$

we chose the following integral path as

$$I(q) = I_{(M)}(q) + I_{(C_+)}(q) + I_{(E)}(q) + I_{(C_-)}(q) = R_+(q) + R_-(q),$$

where  $R_{\pm}(q)$  are residues of the poles enclosed by the integral path, which are given by

$$R_+(q) = i \frac{2i\pi}{2E(q)} \Theta(E_I(q)) = -\frac{\pi}{E(q)} \Theta(E_I(q))$$

and

$$R_-(q) = i \frac{-2i\pi}{-2E(q)} \Theta(E_I(q)) = -\frac{\pi}{E(q)} \Theta(E_I(q)),$$

respectively. Here,  $\Theta(E_I(q))$  is a step function for the imaginary part of the energy. Since  $I_{(C_{\pm})}(q) \rightarrow 0$  for  $\Lambda_0 \rightarrow \infty$ , we have the following relation between the integration of the propagator by the Minkowski momentum  $I_{(M)}(q)$  and that by the Euclidean momentum  $I_{(E)}(q)$  as

$$I_{(M)}(q) = -I_{(E)}(q) + R_+(q) + R_-(q),$$

which gives

$$i \int_{-\infty}^{\infty} dq_0 \frac{1}{q_0^2 - q^2 - M^2(q) + i\varepsilon} = \int_{-\infty}^{\infty} dq_4 \frac{1}{q_4^2 + q^2 + M^2(q) - i\varepsilon} - \frac{2\pi}{E(q)} \Theta(E_I(q)).$$

Defining

$$M_{(M)}(p) \equiv \frac{3\alpha}{4\pi^2} \int dq \frac{q}{p} M_{(M)}(q) I_{(M)}(q) \int_{\eta_-^2}^{\eta_+^2} \frac{dk^2}{k^2 - i\varepsilon}$$

and

$$M_{(E)}(p) \equiv -\frac{3\alpha}{4\pi^2} \int dq \frac{q}{p} M_{(E)}(q) I_{(E)}(q) \int_{\eta_-^2}^{\eta_+^2} \frac{dk^2}{k^2 - i\varepsilon},$$

we have

$$M_{(M)}(p) = M_{(E)}(p) - \frac{3\alpha}{4\pi} \int dq \frac{q}{p} M_{(E)}(q) \left( \frac{2}{E_{(E)}(q)} \Theta((E_{(E)}(q))_I) \right) \int_{\eta_-^2}^{\eta_+^2} \frac{dk^2}{k^2 - i\varepsilon}.$$

Using the relation

$$\Theta((E_{(E)}(q))_I) = \frac{1}{2} \left( 1 + \frac{(E_{(E)}(q))_I}{|(E_{(E)}(q))_I|} \right),$$

we obtain

$$M_{(M)}(p) = \frac{3\alpha}{4\pi} \int dq \frac{q}{p} s_{(E)}(q) M_{(E)}(q) \frac{1}{E_{(E)}(q)} \int_{\eta_-^2}^{\eta_+^2} \frac{dk^2}{k^2 - i\varepsilon}$$

with

$$s_{(E)}(q) = -\frac{(E_{(E)}(q))_I}{|(E_{(E)}(q))_I|}.$$

Here, the solution of  $M_{(E)}(q)$  is obtained by the SDE for the integral path (1) as

$$M_{(E)}(p) = \frac{3\alpha}{4\pi} \int dq \frac{q}{p} M_{(E)}(q) \frac{1}{E_{(E)}(q)} \int_{\eta_-^2}^{\eta_+^2} \frac{dk^2}{k^2 - i\varepsilon},$$

then the energy  $E_{(E)}(q)$  is evaluated with  $M_{(E)}(q)$ . For example, if  $(E_{(E)}(q))_I < 0$  for all  $q$ , we have  $M_{(M)}(p) = M_{(E)}(p)$ . In this case, there are no poles inside the integral path for all  $q$ . Then, the Wick rotation from the real axis to the imaginary axis is valid. Conversely, if  $(E_{(E)}(q))_I > 0$  for all  $q$ , then  $M_{(M)}(p) = -M_{(E)}(p)$ . In this case, there are poles inside the integral path for all  $q$ .

## References

- [1] F.J.Dyson, Phys.Rev.**75** (1949) ,1736.
- [2] J.S.Schwinger,Proc.Nat.Acad.Sci.**37** (1951),452.
- [3] Y. Hayashi and K.-I. Kondo, Phys. Rev. **D103**, L111504 (2021), [arXiv:2103.14322].
- [4] Y. Hayashi and K.-I. Kondo, Phys. Rev.**D104**,074024(2021), [arXiv:2105.07487].
- [5] P. Maris, Phys.Rev.**D50**,4189(1994).
- [6] P. Maris, Phys.Rev.**D52**,6087(1995) [arXiv:hep-ph/9508323].
- [7] P. Maris and H.A.Holties, Int.J.Mod.Phys.**A7** (1992),5369.
- [8] S.Strauss, C.S.Fischer and C.Kellermann, Phys. Rev. Lett. **109** (2012),252001 [arXiv:1208:6239 [hep-ph]].
- [9] C.S.Fischer and M.Q.Huber, Phys. Rev. **D102** (2020),094005 [arXiv:2007.11505].
- [10] N.Dorey and N.E.Mavromatos, Phys.Lett.**B266**, 163(1991).
- [11] K.Fukazawa, T.Inagaki, S.Mukaigawa and T.Muta, Prog. Theor. Phys. **105**,979(2001) [arXiv:hep-ph/9910305].
- [12] D.J.Gross and A.Neveu, Phys. Rev. **D10** (1974),3235.